Eidgenössische Technische Hochschule Zürich
Swiss Federal Institute of Technology Zurich

Seminar for Applied Mathematics SAM

Hagedorn Wavepackets and Schrödinger Equation with Time-Dependent, Homogeneous Magnetic Field

V. Gradinaru and O. Rietmann

Research Report No. 2020-68

November 2020
Latest revision: August 2021

Seminar für Angewandte Mathematik
Eidgenössische Technische Hochschule
CH-8092 Zürich
Switzerland

Hagedorn Wavepackets and Schrödinger Equation with Time-Dependent, Homogeneous Magnetic Field

Vasile Gradinaru, Oliver Rietmann

August 11, 2021

Abstract

Certain generalized coherent states, so-called Hagedorn wavepackets, have been used to numerically solve the standard Schrödinger equation. We extend this approach and its recent enhancements to the magnetic Schrödinger equation for a time-dependent, spatially homogeneous magnetic field. We explain why Hagedorn wavepackets are naturally compatible with the aforementioned physical system. In numerical experiments we examine the order of convergence and the preservation of norm and energy. We use this method to simulate a Penning trap as proposed in recent work on quantum computing.

1 Introduction

The generalized coherent states introduced in [14], nowadays known as Hagedorn wavepackets, have been used successfully to design numerical methods for the Schrödinger equation [9]. The present work adapts the Hagedorn wavepacket approach to the time-dependent Schrödinger equation for a (possibly time dependent) homogeneous magnetic field. More precisely, we extend the recently developed semiclassical splitting methods [11] and its enhancements of high order convergence [3]. We split the original equation into three separate equations. The new part due to the homogeneous magnetic field involves an infinitesimal rotation of the wave function. Then we make two key observations. First, this infinitesimal rotation commutes with the Laplace operator, and thus allows us to decouple the associated time evolutions [12, Sec. 2.1]. Second, the time evolution of the infinitesimal rotation, which is simply a rotation of the wave function, can be expressed naturally in terms of Hagedorn wavepackets. We can retain the high order convergence rates of the zero-field case and need only minor additional effort to treat the new terms in presence of a homogeneous magnetic field. More precisely, we only require the solution of an additional, low dimensional ODE.

Quantum dynamics in presence of magnetic fields is particularly challenging for the space discretisations based on grids. In [12] the authors generalize for instance the well-known Fourier grid approach to the same equation. When charged particles are subject to a homogeneous magnetic field, they start to spin in circles. These rotations can not be expressed exactly on the Fourier grid. However, Hagedorn wavepackets give rise to grid-free methods and can thus overcome this drawback. Additionally, unlike the (discrete) Fourier basis functions, rotated Hagedorn wavepackets are again Hagedorn wavepackets. The time-propagation under the new magnetic field terms can thus be expressed exactly. In general, the Fourier grid approach is complementary to the Hagedorn approach in the

following sense. The Fourier method is satisfactory for large values of the model parameter ε^2, which plays the role of the reduced Planck constant $\hbar$. In contrast, the Hagedorn approach improves for small values of ε^2, i.e. in the semiclassical limit [9]. Moreover, at least for localized (in space and momentum) solutions, the Hagedorn approach is more efficient in high dimensions [9].
Hagedorn wavepackets have been used in [26] to solve the Schrödinger equation for non-homogeneous magnetic fields. The authors thereof mention the semiclassical splitting, but do not aim to generalize it to the magnetic Schrödinger equation. Our work thus differs in the sense that we consider only homogeneous but time dependent magnetic fields and we provide much more efficient methods. In fact, this seems to be the natural way to generalize the semiclassical splitting and its enhancements. For the nonlinear Schrödinger equation, magnetic fields are considered in [10], with a focus on magnetic traps and the rotation they induce.
Homogeneous magnetic fields are used for instance in Penning traps [23, 6, 7] to implement qubits in experimental quantum computing. For instance in [17], the authors consider a Penning trap with a particular homogeneous magnetic field to circumvent some experimental issues. We use this example and (a version of) the Hamiltonian proposed in [17] to conduct our simulations. Thereby we confirm the expected convergence rates of very high order. These simulations involve one or two particles in three dimensions. All our simulation codes are accessible in the repository `https://gitlab.math.ethz.ch/gvasile/WaveBlocksND.git`.

2 The Magnetic Schrödinger Equation

Consider an electric potential $\phi(x,t)$ and a magnetic potential $A(x,t)$, where $x \in \mathbb{R}^d$ and A maps to $\mathbb{R}^d$. We assume that $d \geq 2$. For a spinless[1] particle of unit mass and unit charge, the Hamiltonian reads

$$\begin{aligned} H^\varepsilon &= \tfrac{1}{2}\left(-i\varepsilon^2\nabla - A\right)^2 + \phi \\ &= \tfrac{1}{2}\left(-\varepsilon^4\Delta + 2i\varepsilon^2 A\cdot\nabla + i\varepsilon^2(\nabla\cdot A) + \|A\|^2_{\mathbb{R}^d}\right) + \phi. \end{aligned}$$

The model parameter $\varepsilon^2 > 0$ plays the role of the reduced Planck constant. Now we consider the special case of a homogeneous magnetic field. It is convenient to describe the magnetic potential by a 1-form $A(x,t) = A_l(x,t)\,\mathrm{d}x^l$. The magnetic field being homogeneous then means that the magnetic field 2-form $\mathrm{d}A$ is independent of x. Therefore we choose

$$A(x,t) := B_{jl}(t)\, x^j \mathrm{d}x^l$$

where $B(t) = (B_{jl}(t))_{1\leqslant j,l\leqslant d}$ is a real, skew-symmetric matrix. The corresponding magnetic field 2-form is given by

$$\mathrm{d}A(t) = 2\sum_{1\leqslant j<l\leqslant d} B_{jl}(t)\ \mathrm{d}x^j \wedge \mathrm{d}x^l.$$

We introduce for $j,l \in \{1,\ldots,d\}$ the operators

$$\begin{aligned} p_l^\varepsilon &:= -i\varepsilon^2\partial_l && \text{(components of linear momentum)} \\ L_{jl}^\varepsilon &:= x_j p_l^\varepsilon - x_l p_j^\varepsilon && \text{(generalized angular momentum)} \end{aligned}$$

[1] We treat only spinless particles and refer to [12, Sec. 3.1] for an explaination on how to add spin in the case of a single particle in a homogenous magnetic field.

and

$$H_B^\varepsilon(t) := -\sum_{1\leqslant j<l\leqslant d} B_{jl}(t) L_{jl}^\varepsilon. \tag{2.1}$$

For this particular vector potential, we have

$$i\varepsilon^2 A\cdot\nabla = H_B^\varepsilon(t), \quad (\nabla\cdot A)\equiv 0, \quad \tfrac{1}{2}\|A\|_{\mathbb{R}^d}^2 = \tfrac{1}{2}\|B(t)x\|_{\mathbb{R}^d}^2$$

and our Hamiltonian thus reads [22]

$$H^\varepsilon = \underbrace{-\tfrac{\varepsilon^4}{2}\Delta}_{T:=} + \underbrace{H_B^\varepsilon(t)}_{M:=} + \underbrace{\tfrac{1}{2}\|B(t)x\|_{\mathbb{R}^d}^2 + \phi(x,t)}_{V:=}. \tag{2.2}$$

The associated Schrödinger equation is given by

$$i\varepsilon^2\partial_t\psi(x,t) = H^\varepsilon\psi(x,t), \quad \psi(x,t_0) = \psi_0(x). \tag{2.3}$$

Let us label the separate equations:

$$i\varepsilon^2\partial_t\psi(x,t) = T\psi(x,t) \tag{T}$$
$$i\varepsilon^2\partial_t\psi(x,t) = M\psi(x,t) \tag{M}$$
$$i\varepsilon^2\partial_t\psi(x,t) = V\psi(x,t) \tag{V}$$

Compared to the standard Schrödinger equation (zero magnetic field), we get an additional quadratic potential term and an advection term $H_B^\varepsilon(t)$. The time evolution of Equation (M) is simply a rotation of the wave function that depends on the magnetic field $B(t)$. More precisely, consider the ODE

$$\tfrac{\mathrm{d}}{\mathrm{d}t}y(t) = B(t)y(t). \tag{B}$$

By [24, Thm X.69] there exists a rotation $R(t,t_0)\in \mathrm{SO}(d)$ such that $y(t) = R(t,t_0)y(t_0)$ solves (B) and $R(t_0,t_0) = \mathrm{id}$, that is $R(t,t_0)$ is the flow map associated with (B). Then the wave function

$$\psi(x,t) = \Phi_M(t,t_0)\psi_0(x) := \psi_0\left(R^T(t,t_0)x\right) \tag{2.4}$$

solves the magnetic equation (M) [12, Lem 2.1] and the corresponding unitary propagator is denoted by $\Phi_M(t,t_0)$. Note that the ODE (B) is independent of the model parameter ε. In our simulations, we approximate the rotation $R(t,t_0)$ by a truncated Magnus expansion. See Section 5.5 for the precise method. Finally, we observe a crucial structure of our equation

$$H^\varepsilon = \underbrace{T+M}_{\text{commute}} + V.$$

The unitary propagators associated with the Hamiltonians T and M commute [12, Lem 2.3]. The flow map associated with the Hamiltonian $T+M$ thus reads

$$\Phi_{T+M}(t,t_0) = \Phi_T(t,t_0)\circ\Phi_M(t,t_0) = \Phi_M(t,t_0)\circ\Phi_T(t,t_0), \tag{2.5}$$

where

$$\Phi_T(t,t_0) = e^{-i\varepsilon^2(t-t_0)(-\Delta)/2}.$$

3 Hagedorn Wavepackets

In [12], a Fourier grid approach is used to numerically solve Equation (2.3). It uses dense grids and thus becomes very expensive for dimensions $d > 3$. The Hagedorn wavepackets are sparser and thus better suited in high dimensions. Moreover, as Equation (2.4) indicates, suitiable basis functions should be compatible with rotations. While this is not the case for the Fourier basis functions, Lemma 1 below asserts that Hagedorn wavepackets can be rotated naturally, and thus motivates their use in the context of magnetic fields. The Hagedorn wavepackets were developed in [13] and [14]. However, we use the notation of [9]. Let $q, p \in \mathbb{R}^d$ and $Q, P \in \mathbb{C}^{d\times d}$ with

$$Q^T P - P^T Q = 0, \quad Q^* P - P^* Q = 2i\,\mathrm{id}, \tag{3.1}$$

where Q^* denotes conjugate-transpose and Q^T denotes transpose without complex conjugation. Moreover, we abbreviate $\Pi := (q, p, Q, P)$. Using the vector-valued raising and lowering operators

$$\begin{aligned}\mathcal{R}^\varepsilon[\Pi] &:= \frac{i}{\sqrt{2\varepsilon^2}}\left(P^*(x-q) - Q^*\left(-i\varepsilon^2\nabla_x - p\right)\right)\\ \mathcal{L}^\varepsilon[\Pi] &:= -\frac{i}{\sqrt{2\varepsilon^2}}\left(P^T(x-q) - Q^T\left(-i\varepsilon^2\nabla_x - p\right)\right)\end{aligned}$$

we define for $k \in \mathbb{N}_0^d$ the Hagedorn wavepackets $\varphi_k^\varepsilon[\Pi]$ recursively by

$$\varphi_0^\varepsilon[\Pi](x) := \left(\pi\varepsilon^2\right)^{-\frac{d}{4}} (\det Q)^{-\frac{1}{2}} \exp\left(\tfrac{i}{2\varepsilon^2}(x-q)^T PQ^{-1}(x-q) + \tfrac{i}{\varepsilon^2}p^T(x-q)\right)$$

and

$$\varphi_{k+e_j}^\varepsilon[\Pi] := \tfrac{1}{\sqrt{k_j+1}}\mathcal{R}_j^\varepsilon[\Pi]\,\varphi_k^\varepsilon[\Pi] \tag{3.2}$$

for all $k \in \mathbb{N}_0^d$ and all $j \in \{1, \dots, d\}$. The functions obtained in this way form an orthonormal basis of $L^2\left(\mathbb{R}^d\right)$, see [14]. To get familiar with the notation, we consider an example in $d = 2$ dimensions.

Example 1. *The parameters $\Pi_0 := (q_0, p_0, Q_0, P_0)$ with*

$$q_0 = (0,0), \quad p_0 = (0,0), \quad Q_0 = \mathrm{id}_{\mathbb{R}^2}, \quad P_0 = i\,\mathrm{id}_{\mathbb{R}^2}$$

satisfy the condition (3.1). We have

$$\varphi_{(0,0)}^\varepsilon[\Pi_0](x) = \left(\pi\varepsilon^2\right)^{-\frac{1}{2}} e^{-\frac{1}{2\varepsilon^2}x^T x}$$

and the j-th component of the raising operator $\mathcal{R}^\varepsilon[\Pi_0]$ reads

$$\mathcal{R}_j^\varepsilon[\Pi_0] = \frac{i}{\sqrt{2\varepsilon^2}}\left(-ix_j + i\varepsilon^2\partial_j\right).$$

Using this expression with $j = 1$ we arrive at

$$\varphi_{(1,0)}^\varepsilon[\Pi_0](x) = \mathcal{R}_1^\varepsilon[\Pi_0]\,\varphi_{(0,0)}^\varepsilon[\Pi_0](x) = \tfrac{2}{\sqrt{2\pi\varepsilon^2}}x_1 e^{-\frac{1}{2\varepsilon^2}x^T x}.$$

Similarly, one can compute

$$\begin{aligned}\varphi_{(0,1)}^\varepsilon[\Pi_0](x) &= \mathcal{R}_2^\varepsilon[\Pi_0]\,\varphi_{(0,0)}^\varepsilon[\Pi_0](x) = \tfrac{2}{\sqrt{2\pi\varepsilon^2}}x_2 e^{-\frac{1}{2\varepsilon^2}x^T x}\\ \varphi_{(1,1)}^\varepsilon[\Pi_0](x) &= \mathcal{R}_2^\varepsilon[\Pi_0]\,\varphi_{(1,0)}^\varepsilon[\Pi_0](x) = \tfrac{2}{\sqrt{\pi\varepsilon^3}}x_1 x_2 e^{-\frac{1}{2\varepsilon^2}x^T x}\\ \varphi_{(2,1)}^\varepsilon[\Pi_0](x) &= \tfrac{1}{\sqrt{2}}\mathcal{R}_1^\varepsilon[\Pi_0]\,\varphi_{(1,1)}^\varepsilon[\Pi_0](x) = \tfrac{1}{\sqrt{\pi\varepsilon^4}}\left(2x_1^2 - \varepsilon^2\right)x_2 e^{-\frac{1}{2\varepsilon^2}x^T x}.\end{aligned}$$

We represent the solution of (2.3) in terms of such Hagedorn wavepackets multiplied by a phase factor

$$\psi(x,t) = e^{iS(t)/\varepsilon^2} \sum_{k\in\mathcal{K}} c_k(t)\, \varphi_k^\varepsilon[\Pi(t)](x), \tag{3.3}$$

where $S(t)$ is a real-valued function and $\mathcal{K} \subset \mathbb{N}_0$ is a multi-index set. In the numerical simulations of Section 5, we choose [9, Sec.5.4]

$$\mathcal{K} = \left\{ k \in \mathbb{N}_0^d \,|\, \prod_{j=1}^d (1+k_j) \leq K \right\} \tag{3.4}$$

with some truncation constant $K \in \mathbb{N}$. Equation (2.4) asserts that if we can rotate Hagedorn wavepackets, then we can also propagate them according to (M).

Lemma 1. *Let $\Pi := (q,p,Q,P)$ satisfy (3.1) and let $R \in \mathrm{SO}(d)$. Then the rotated parameters*

$$R\Pi := (Rq, Rp, RQ, RP)$$

still satisfy (3.1) and we have

$$\varphi_k^\varepsilon[\Pi]\left(R^T x\right) = \varphi_k^\varepsilon[R\Pi](x) \tag{3.5}$$

for all $\varepsilon > 0$ and all $k \in \mathbb{N}_0^d$.

Proof. We fix $R \in \mathrm{SO}(d)$ and show the formula by induction on $k \in \mathbb{N}_0^d$. For $k = 0$, this is straightforward to verify. Let $\rho(R)$, be the map that rotates functions by R, i.e.

$$\rho(R)\varphi(x) = \varphi\left(R^T x\right)$$

for all $\varphi \in L^2\left(\mathbb{R}^d;\mathbb{C}\right)$. The next step is to show that

$$\rho(R)\mathcal{R}^\varepsilon[\Pi] = \mathcal{R}^\varepsilon[R\Pi]\rho(R). \tag{3.6}$$

To this end, let $\varphi : \mathbb{R}^d \to \mathbb{C}$ be a smooth function. By chain rule, we have

$$\nabla_x\left(\varphi\left(R^T x\right)\right) = R\left(\nabla_x\varphi\right)\left(R^T x\right).$$

It follows that

$$\left(Q^*\left(-i\varepsilon^2\nabla_x - p\right)\varphi\right)\left(R^T x\right) = (RQ)^*\left(-i\varepsilon^2\nabla_x - Rp\right)\varphi\left(R^T x\right).$$

Together with

$$P^*\left(R^T x - q\right)\varphi\left(R^T x\right) = (RP)^*(x - Rq)\,\varphi\left(R^T x\right),$$

this proves (3.6). Finally, we fix $j \in \{1,\ldots,d\}$ and compute

$$\begin{aligned}
\sqrt{k_j+1}\rho(R)\varphi_{k+e_j}^\varepsilon[\Pi] &\overset{(3.2)}{=} \rho(R)\mathcal{R}_j^\varepsilon[\Pi]\varphi_k^\varepsilon[\Pi] \\
&\overset{(3.6)}{=} \mathcal{R}_j^\varepsilon[R\Pi]\rho(R)\varphi_k^\varepsilon[\Pi] \\
&\overset{(3.5)}{=} \mathcal{R}_j^\varepsilon[R\Pi]\varphi_k^\varepsilon[R\Pi] \\
&\overset{(3.2)}{=} \sqrt{k_j+1}\varphi_{k+e_j}^\varepsilon[R\Pi],
\end{aligned}$$

where we used the induction hypothesis in the third step. This proves (3.5). It is straight forward to check that the rotated parameters satisfy (3.1). □

If we apply this result to $R = R(t,t_0)$ as in (2.4), we obtain the time evolution of $\psi(x,t)$ in (3.3) under (M). The exact time evolution under (M) has been pointed out in [14, Thm 3.4], but without link to rotations (as it covers a more general case).

4 Semiclassical Splitting

We extend the semiclassical splitting developed in [9] and [11] to the Hamiltonian (2.2). We represent our approximate solution $\psi(t)$ by a Hagedorn wavepacket as in (3.3). Propagating $\psi(t)$ means propagating its parameters $S(t), \Pi(t) := (q(t), p(t), Q(t), P(t))$ and its coefficients $c_k(t), k \in \mathcal{K}$. The precise algorithm for this propagation goes as follows. We assume for simplicity that our Hamiltonian (2.2) is time-independent, i.e. that M and V are time-independent. In Section 5.4 we extend all the schemes discussed below to the non-autonomous case. We split the Schrödinger equation into two parts

$$\dot{\psi}(t) = \mathcal{A}(t)\psi(t) + \mathcal{B}(t)\psi(t), \quad \psi(0) = \psi_0 \tag{4.1}$$

with

$$\mathcal{A}(t) = -\tfrac{i}{\varepsilon^2}(T + M + U(x,t)) \quad \text{and} \quad \mathcal{B}(t) = -\tfrac{i}{\varepsilon^2}W(x,t).$$

Here, we have

$$V(x,t) = U(x,t) + W(x,t),$$

where $U(x,t)$ is the local quadratic Taylor expansion of $V(x)$ at position $q = q(t)$, and $W(x,t)$ is the non-quadratic remainder. More precisely, we have

$$U(x,t) = V(q) + \nabla V(q)\cdot(x-q) + \tfrac{1}{2}(x-q)^T \nabla^2 V(q)(x-q),$$

where $\nabla^2 V$ denotes the Hessian of V, and

$$W(x,t) = V(x) - U(x,t).$$

The *semiclassial splitting* for a time step $[0,h]$ is

$$\exp\left(\tfrac{h}{2}\mathcal{A}\left(\tfrac{h}{2}\right)\right)\exp\left(h\mathcal{B}\left(\tfrac{h}{2}\right)\right)\exp\left(\tfrac{h}{2}\mathcal{A}(0)\right). \tag{4.2}$$

In the next two sections, we specify how these exponentials act on ψ_0, i.e. on its parameters and coefficients. See also the pseudo code in Algorithm 1 below.

4.1 Propagation with Respect to $\mathcal{A}$

To solve the equation

$$\dot{\psi}(t) = \mathcal{A}(t)\psi(t), \quad \psi(0) = \psi_0, \tag{4.3}$$

we split it into

$$\dot{\psi}(t) = -\tfrac{i}{\varepsilon^2}(T+M)\psi(t) \qquad \text{and} \qquad \dot{\psi}(t) = -\tfrac{i}{\varepsilon^2}U(x,t)\psi(t). \tag{4.4}$$

Both of these equations can be solved exactly.

Remark 1. *The exact time evolution under each of these equations preserves the Hagedorn wavepackets in the following sense. Suppose we take as initial data just a single Hagedorn basis function*

$$e^{iS(0)/\varepsilon^2}\varphi_j^\varepsilon[\Pi(0)]$$

for some multi-index $j \in \mathbb{N}_0^d$. Then the solution according to both equations will be of the form

$$e^{iS(t)/\varepsilon^2}\varphi_j^\varepsilon[\Pi(t)]$$

for all times $t > 0$, where the parameters S and Π satisfy a certain ODE to be specified below. In particular, the coefficients c_k in the basis expansion (3.3) remain constant under these time evolutions.

This result is due to [14]. The assumption that the magnetic field is homogeneous (but possibly time-dependent) is crucial for this property. Below, we give these ODEs and their exact solutions for the parameters. We then concatenate these exact solutions to an approximate solution of (4.3) by a splitting. We call this the *inner* splitting.

(i) The Hagedorn wavepacket ψ solves the first equation in (4.4) if its coefficients remain constant and its parameters satisfy the ODE [14]

$$\begin{aligned}
\dot{q}(t) &= p(t) + Bq(t) \\
\dot{p}(t) &= Bp(t) \\
\dot{Q}(t) &= P(t) + BQ(t) \\
\dot{P}(t) &= BP(t) \\
\dot{S}(t) &= \tfrac{1}{2}\|p(t)\|_{\mathbb{R}^d}^2.
\end{aligned} \tag{4.5}$$

The exact solution for a time step δt is given by

$$\begin{aligned}
q(\delta t) &= \exp(\delta t \cdot B)(q(0) + \delta t \cdot p(0)) \\
p(\delta t) &= \exp(\delta t \cdot B)\, p(0) \\
Q(\delta t) &= \exp(\delta t \cdot B)(Q(0) + \delta t \cdot P(0)) \\
P(\delta t) &= \exp(\delta t \cdot B)\, P(0) \\
S(\delta t) &= S(0) + \delta t \cdot \tfrac{1}{2}\|p(0)\|_{\mathbb{R}^d}^2.
\end{aligned}$$

Note that this is just a concatenation of the flow maps associated with T and M, which in turn is just Equation (2.5) on the level of parameters. Since we assume that B is time-independent, the matrix $R(t, t_0)$ in (2.4) corresponds to $R(\delta t, 0) = \exp(\delta t \cdot B)$.

(ii) The Hagedorn wavepacket ψ solves the second equation in (4.4) if its coefficients remain constant and its parameters satisfy the ODE [14]

$$\begin{aligned}
\dot{q}(t) &= 0 \\
\dot{p}(t) &= -\nabla U(q(t), t) \\
\dot{Q}(t) &= 0 \\
\dot{P}(t) &= -\nabla^2 U(q(t), t)\, Q(t) \\
\dot{S}(t) &= -U(q(t), t)
\end{aligned}$$

The exact solution for a time step δt is given by

$$\begin{aligned}
q(\delta t) &= q(0) \\
p(\delta t) &= p(0) - \delta t \cdot \nabla U(q(0), 0) \\
Q(\delta t) &= Q(0) \\
P(\delta t) &= P(0) - \delta t \cdot \nabla^2 U(q(0), 0)\, Q(0) \\
S(\delta t) &= S(0) - \delta t \cdot U(q(0), 0).
\end{aligned}$$

We concatenate the exact propagations (i) and (ii) to an approximate the solution of (4.2) using N steps of the splitting of order 8 from [18], see also [15, Eq. 3.14]. For details on this splitting, see Algorithm 2 and Table 1 below. The size of a single step of this inner

splitting is $\delta t = h/N$, where h is the external time step from (4.2). The number of inner time steps for the semiclassical splitting is [11]

$$N = 1 + \left\lfloor \varepsilon^{-\frac{3}{8}} h^{\frac{3}{4}} \right\rfloor. \tag{4.6}$$

This choice results in a convergence rate of εh^2 for the overall method (4.2) as explained in Section 4.3.

4.2 Propagation with Respect to $\mathcal{B}$

It remains to solve the equation of the non-quadratic remainder, that is

$$\dot{\psi}(t) = \mathcal{B}(t)\psi(t), \quad \psi(0) = \psi_0, \tag{4.7}$$

or equivalently

$$\dot{\psi}(x,t) = -\tfrac{i}{\varepsilon^2} W(x,t)\psi(x,t), \quad \psi(0) = \psi_0.$$

This is done exactly as in the zero magnetic field case, see [9, Sec.2.5]. We compute the Galerkin matrix of $W(x,0)$ w.r.t. the Hagedorn wavepacket basis

$$F_{j,k}[\Pi(0)] = \int_{\mathbb{R}^d} \overline{\varphi_j^\varepsilon[\Pi(0)](x)} W(x,0)\, \varphi_k^\varepsilon[\Pi(0)](x)\,\mathrm{d}x, \quad j,k \in \mathcal{K}. \tag{4.8}$$

This yields an ODE for the coefficients $(c_k(t))_{k\in\mathcal{K}}$, namely

$$i\varepsilon^2 \dot{c}(t) = F[\Pi(0)]\, c(t).$$

An approximate time step $[0,h]$ according (4.7) then reads

$$c(h) = \exp\left(-\frac{i}{\varepsilon^2} h F[\Pi(0)]\right) c(0)$$

and the parameters $\Pi(t)$ and $S(t)$ stay unaltered. As in [3], we point out the following: The remainder W perturbs the solution w.r.t. $\mathcal{A}$ by order $\mathcal{O}(\varepsilon^3)$ as $\varepsilon \to 0$ (see [11, Lem. 3]). This will be used in Section 5.

Algorithm 1 semiclassical_splitting

Input: final time t; number of outer time steps n; initial parameters Π, S; initial coefficients $c = (c_k)_{k\in\mathcal{K}}$;

Output: Parameters Π, S and coefficients c at final time;

```
h := t/n
for j = 0 to n − 1 do
    Π, S = inner_splitting(h/2, Π, S)
    F[Π] = Galerkin matrix in (4.8)
    c = exp(−(ih/ε²) F[Π]) c
    Π, S = inner_splitting(h/2, Π, S)
end for
return Π, S, c
```

Algorithm 2 inner_splitting

Input: final time h; initial parameters Π, S

Output: Parameters Π, S at final time $\delta t \cdot N$;

$N := \lceil 1 + \varepsilon^{-\frac{3}{4}} \sqrt{h} \rceil$
$\delta t := h/N$
$L := 18$
Set $a_1, \ldots, a_L$ and $b_1, \ldots, b_L$ as in Table 1
for $j = 0$ to $N - 1$ **do**
  for $l = 1$ to L **do**
    $\Pi, S =$ Exact propagation of (Π, S) by $a_l \cdot \delta t$ using (i)
    $\Pi, S =$ Exact propagation of (Π, S) by $b_l \cdot \delta t$ using (ii)
  end for
end for
return Π, S

$a_1 = 0$	$a_2 = 0.13020248308889007$	$a_3 = 0.5611629817751084$
$a_4 = -0.38947496264484727$	$a_5 = 0.1588419065551556$	$a_6 = -0.39590389413323757$
$a_7 = 0.1845396409783157$	$a_8 = 0.25837438768632204$	$a_9 = 0.2950117236093103$
$a_{10} = -0.6055085338300346$	$a_{11} = 0.2950117236093103$	$a_{12} = 0.25837438768632204$
$a_{13} = 0.1845396409783157$	$a_{14} = -0.39590389413323757$	$a_{15} = 0.1588419065551556$
$a_{16} = -0.38947496264484727$	$a_{17} = 0.5611629817751084$	$a_{18} = 0.13020248308889007$
$b_1 = 0.06510124154444503$	$b_2 = 0.3456827324319992$	$b_3 = 0.08584400956513055$
$b_4 = -0.11531652804484582$	$b_5 = -0.118530993789041$	$b_6 = -0.1056821265774609$
$b_7 = 0.22145701433231887$	$b_8 = 0.27669305564781616$	$b_9 = -0.15524840511036214$
$b_{10} = -0.15524840511036214$	$b_{11} = 0.27669305564781616$	$b_{12} = 0.22145701433231887$
$b_{13} = -0.1056821265774609$	$b_{14} = -0.118530993789041$	$b_{15} = -0.11531652804484582$
$b_{16} = 0.08584400956513055$	$b_{17} = 0.3456827324319992$	$b_{18} = 0.06510124154444503$

Table 1: Coefficients for the splitting of order 8 from [18].

4.3 Convergence Estimates and the Choice of N

The choice of the number of inner time steps N in (4.6) is motivated by the convergence estimates from [11, Sec. 3] for the zero magnetic field case. However, [11] only covers the case $d = 1$ (dimension one). This rules out the magnetic field since the only skew-symmetric 1×1 matrix is $B = 0$, which results in $M = 0$. The estimates in [11, Sec. 3] remain valid in higher dimensions, but the computations are much more involved. On the other hand, the presence of a magnetic field does not affect the arguments in [11, Sec. 3]. The reason is that the magnetic field only affects the ODEs in Items (i) and (ii) and these can still be solved exactly. In fact, we could replace these ODEs with any other. As long as we can solve both of them exactly, the estimates in [11, Sec. 3] remain valid. In Theorem 1 below, we formulate the convergence estimates for the semiclassical splitting in the presence of a magnetic field and in dimensions $d \geq 2$. But for the sake of brevity, we will only outline the proof. Suppose that $\psi(t) \in L^2\left(\mathbb{R}^d\right)$ is the exact solution of the

initial value problem (4.1) at time t, that is

$$\psi(x,t) = e^{iS(t)/\varepsilon^2} \sum_{k\in\mathbb{N}_0^d} c_k(t)\, \varphi_k^\varepsilon[\Pi(t)](x),$$

where $S(t), \Pi(t)$ and $c(t)$ are now the parameters and coefficients of the exact solution at time t. Moreover, we introduce the K-truncation of the exact solution (see (3.4))

$$u(x,t) = e^{iS(t)/\varepsilon^2} \sum_{k\in\mathcal{K}} c_k(t)\, \varphi_k^\varepsilon[\Pi(t)](x).$$

The parameters and coefficients of the approximate solution $\tilde{u}$ according to the semiclassical splitting (4.2) are denoted with a tilde superscript, i.e.

$$\tilde{u}(x,t) = e^{i\tilde{S}(t)/\varepsilon^2} \sum_{k\in\mathcal{K}} \tilde{c}_k(t)\, \varphi_k^\varepsilon\left[\tilde{\Pi}(t)\right](x).$$

We assume that the initial parameters agree, that is $S(0) = \tilde{S}(0)$ and $\Pi(0) = \tilde{\Pi}(0)$.

Theorem 1. *As above, let ψ, u and $\tilde{u}$ denote the exact, the K-truncated and the approximate solution to the initial value problem (4.1). Then for all $t > 0$, there exists a constant $C > 0$ such that*

$$\|\psi(t) - \tilde{u}(t)\|_{L^2} \le \|\psi(t) - u(t)\|_{L^2} + C\varepsilon h^2,$$

where h is the outer time step size in (4.2). The constant C does not depend on $h, \delta t$ or ε, but depends on the truncation constant K and on the time interval $[0,t]$.

Sketch of proof. Using the triangle inequality, we find

$$\|\psi(t) - \tilde{u}(t)\|_{L^2} \le \|\psi(t) - u(t)\|_{L^2} + \|u(t) - \tilde{u}(t)\|_{L^2}.$$

To estimate the second term on the right-hand side, we focus on a single outer time step h and introduce the intermediate solution

$$u_1(x,h) = e^{iS(h)/\varepsilon^2} \sum_{k\in\mathcal{K}} c_k^1(h)\, \varphi_k^\varepsilon[\Pi(h)](x),$$

where $\Pi^1 := \Pi\left(\frac{h}{2}\right)$ and

$$i\varepsilon^2 \dot{c}^1 = F\left[\Pi^1\right] c^1.$$

Hence u_1 has the exact parameters but only approximate coefficients. The triangle inequality yields

$$\|u(h) - \tilde{u}(h)\|_{L^2} \le \|u(h) - u_1(h)\|_{L^2} + \|u_1(h) - \tilde{u}(h)\|_{L^2}.$$

We estimate the two terms on the left-hand side by Theorem 3 and the right-hand side by Lemma 4 in [11] and obtain

$$\|u(h) - u_1(h)\|_{L^2} \le C_1\varepsilon h^3 \qquad \text{and} \qquad \|u_1(h) - \tilde{u}(h)\|_{L^2} \le C_2 \frac{(\delta t)^8}{\varepsilon^2} h, \tag{4.9}$$

where δt denotes the inner time step. If we choose N like in (4.6), we have

$$\delta t \le \varepsilon^{\frac{3}{8}} h^{\frac{1}{4}}$$

and consequently

$$\|u_1(h) - \tilde{u}(h)\|_{L^2} \leq C_2 \frac{(\delta t)^8}{\varepsilon^2} h \leq C_2 \varepsilon h^3. \tag{4.10}$$

By a standard Lady Windermere's fan argument, we obtain [11, Thm. 1]

$$\|\psi(t) - \tilde{u}(t)\|_{L^2} \leq \|\psi(t) - u(t)\|_{L^2} + C\varepsilon h^2.$$

□

Remark 2. *The choice of N in (4.6) is adapted to the semiclassical splitting. The higher order splittings of the next section require a different choice of N. In order to achieve the bound*

$$\|u_1(h) - \tilde{u}(h)\|_{L^2} \leq C_2 \varepsilon^\alpha h^{\beta+1},$$

we need to choose [11]

$$N = 1 + \left\lfloor \left(\frac{h^{8-\beta}}{\varepsilon^{2+\alpha}} \right)^{\frac{1}{8}} \right\rfloor. \tag{4.11}$$

For example, we used $\alpha = 1$ and $\beta = 2$ above to match the two error bounds in (4.9).

Remark 3. *The truncation error $\|\psi(t) - u(t)\|_{L^2}$ in Theorem 1 can be made arbitrarily small by choosing K sufficiently large. In the simulations, one has to a priori guess an appropriate value for K, so that the K-truncated Hagedorn basis contains the exact solution over the whole simulation time. The truncation error is then not visible in the convergence plot, see Section 6 for some examples. In general, the larger ε and the more the solution is spread out in phase space, the larger we need to choose K.*

5 Higher Order Splitting Schemes

In [3, Sec. 3], the authors present several improvements of the semiclassical splitting for the standard Schrödinger equation, i.e. without magnetic field. The goal of this section is to explain how all of these improvements can be naturally generalized to the case with magnetic field. We closely follow [3, Sec. 3] and consider a differential equation of the form

$$\dot{\psi} = \mathcal{A}\psi + \mathcal{B}\psi, \quad \psi(t_0) = \psi_0$$

with the (time-independent) vector fields $\mathcal{A}$ and $\mathcal{B}$. We denote the corresponding flow maps with time step $h \in \mathbb{R}$ by $e^{h\mathcal{A}}$ and $e^{h\mathcal{B}}$. Moreover, we slightly abuse this notation and keep writing exponentials for the flow maps even if the operators $\mathcal{A}$ and $\mathcal{B}$ depend on time. For splitting coefficients $a, b \in \mathbb{R}^s$, we denote the corresponding splitting scheme by

$$e^{h\mathcal{B}} \overset{(b,a)}{\circ} e^{h\mathcal{A}} = e^{b_s h\mathcal{B}} \circ e^{a_s h\mathcal{A}} \circ \cdots \circ e^{b_1 h\mathcal{B}} \circ e^{a_1 h\mathcal{A}}. \tag{5.1}$$

In the context of Lie-operators, one sometimes follows the convention that the operators are applied in the reverse order than they are written, see for example [1, Sec. A.1]. But we will not follow this convention. For example in (5.1), the rightmost operator is applied first.

5.1 Splittings for Perturbed Systems

A consistent splitting scheme takes the form

$$e^{h\mathcal{B}} \overset{(b,a)}{\circ} e^{h\mathcal{A}} = \exp\left(h\left(\mathcal{A}+\mathcal{B}+E\left(h\right)\right)\right),$$

with remainder

$$\begin{aligned} E\left(h\right) = {} & h\nu_{ab}\left[\mathcal{A},\mathcal{B}\right] + h^2\nu_{aab}\left[\mathcal{A},\left[\mathcal{A},\mathcal{B}\right]\right] + h^2\nu_{bab}\left[\mathcal{B},\left[\mathcal{A},\mathcal{B}\right]\right] \\ & + h^3\nu_{aaab}\left[\mathcal{A},\left[\mathcal{A},\left[\mathcal{A},\mathcal{B}\right]\right]\right] + h^3\nu_{baab}\left[\mathcal{B},\left[\mathcal{A},\left[\mathcal{A},\mathcal{B}\right]\right]\right] \\ & + h^3\nu_{bbab}\left[\mathcal{B},\left[\mathcal{B},\left[\mathcal{A},\mathcal{B}\right]\right]\right] + \mathcal{O}\left(h^4\right) \end{aligned}$$

Suppose now that the vector field $\mathcal{B}$ is merely a perturbation of $\mathcal{A}$, say $\mathcal{B} = \varepsilon\mathcal{B}_0$ for some small $\varepsilon > 0$ and a vector field $\mathcal{B}_0$ of same scale as $\mathcal{A}$. Then the remainder becomes

$$\begin{aligned} E\left(h,\varepsilon\right) = {} & h\varepsilon\nu_{ab}\left[\mathcal{A},\mathcal{B}_0\right] + h^2\varepsilon\nu_{aab}\left[\mathcal{A},\left[\mathcal{A},\mathcal{B}_0\right]\right] + h^2\varepsilon^2\nu_{bab}\left[\mathcal{B}_0,\left[\mathcal{A},\mathcal{B}_0\right]\right] \\ & + h^3\varepsilon\nu_{aaab}\left[\mathcal{A},\left[\mathcal{A},\left[\mathcal{A},\mathcal{B}_0\right]\right]\right] + h^3\varepsilon^2\nu_{baab}\left[\mathcal{B}_0,\left[\mathcal{A},\left[\mathcal{A},\mathcal{B}_0\right]\right]\right] \\ & + h^3\varepsilon^3\nu_{bbab}\left[\mathcal{B}_0,\left[\mathcal{B}_0,\left[\mathcal{A},\mathcal{B}_0\right]\right]\right] + \mathcal{O}\left(h^4\right). \end{aligned}$$

As in [20], we say the method (5.1) is of generalized order $(r_1, r_2, \ldots, r_m)$, where $r_1 \geq r_2 \geq \cdots \geq r_m$, if the remainder satisfies

$$E\left(h,\varepsilon\right) = \mathcal{O}\left(\varepsilon h^{r_1} + \varepsilon^2 h^{r_2} + \cdots + \varepsilon^m h^{r_m}\right).$$

The choice $a = \left(\frac{1}{2}, \frac{1}{2}\right)$ and $b = (1, 0)$ leads to the well-known *Strang splitting* [25], which is of order 2. Now we give two examples of perturbation aware splittings, both taken from [20]. First, we consider the symmetric, splitting of generalized order $(4, 2)$

$$\Psi_{(4,2)}\left(h\right) = e^{a_1 h\mathcal{A}} e^{b_1 h\mathcal{B}} e^{a_2 h\mathcal{A}} e^{b_1 h\mathcal{B}} e^{a_1 h\mathcal{A}}, \tag{5.2}$$

with $a_1 = \frac{1}{6}\left(3-\sqrt{3}\right), a_2 = 1-2a_1, b_1 = \frac{1}{2}$. In Remark 2 we choose $\alpha = 2$ and $\beta = 2$, which yields for the number of inner time steps

$$N = 1 + \left\lfloor \varepsilon^{-\frac{1}{2}} h^{\frac{3}{4}} \right\rfloor.$$

This yields the desired generalized convergence rate $(4, 2)$. Second, we consider the method of generalized order $(8, 4)$ given by

$$\Psi_{(8,4)}\left(h\right) = e^{a_1 h\mathcal{A}} e^{b_1 h\mathcal{B}} e^{a_2 h\mathcal{A}} e^{b_2 h\mathcal{B}} e^{a_3 h\mathcal{A}} e^{b_3 h\mathcal{B}} e^{a_3 h\mathcal{A}} e^{b_2 h\mathcal{B}} e^{a_2 h\mathcal{A}} e^{b_1 h\mathcal{B}} e^{a_1 h\mathcal{A}}, \tag{5.3}$$

with coefficients given in Table 2. In Remark 2 we choose $\alpha = 2$ and $\beta = 4$, which yields

$a_1 = 0.0753469602698929$	$a_2 = 0.5179168546882568$	$a_3 = \frac{1}{2} - (a_1 + a_2)$
$b_1 = 0.1902259393736766$	$b_2 = 0.8465240704435263$	$b_3 = 1 - 2\left(b_1 + b_2\right)$

Table 2: Coefficients for the $(8, 4)$ symmetric splitting [20].

for the number of inner time steps

$$N = 1 + \left\lfloor \sqrt{\frac{h}{\varepsilon}} \right\rfloor.$$

This yields the desired generalized convergence rate $(8, 4)$.

5.2 Processed Methods for Perturbed Systems

In this section, we improve our splitting schemes using a *pre-processor*. This is a map $\pi_h : L^2\left(\mathbb{R}^d\right) \to L^2\left(\mathbb{R}^d\right)$, such that the method

$$\widetilde{\Psi}(h) = \pi_h \circ \Psi(h) \circ \pi_h^{-1},$$

is more accurate than $\Psi(h)$. The n-fold concatenation $\widetilde{\Psi}^n(h)$ of the processed method then satisfies $\widetilde{\Psi}^n(h) = \pi_h \circ \Psi^n(h) \circ \pi_h^{-1}$. Thus it is as expensive as the n-fold concatenation $\Psi^n(h)$ of the non-processed method and still more accurate. In our simulations, we will examine the processed method of generalized order $(7, 6, 4)$ from [2] given by

$$\widetilde{\Psi}_{(7,6,4)}(h) = \left(e^{h\mathcal{A}} \overset{(z,y)}{\circ} e^{h\mathcal{B}}\right) \circ \left(e^{h\mathcal{B}} \overset{(b,a)}{\circ} e^{h\mathcal{A}}\right) \circ \left(e^{-h\mathcal{B}} \overset{(y,z)}{\circ} e^{-h\mathcal{A}}\right), \tag{5.4}$$

with coefficients given in Table 3. In Remark 2 we choose $\alpha = 3$ and $\beta = 4$, which yields

$a_1 = 0.5600879810924619$	$a_2 = \frac{1}{2} - a_1$	
$b_1 = 1.5171479707207228$	$b_2 = 1 - 2b_1$	
$z_1 = -0.3346222298730800$	$z_2 = 1.0975679907321640$	$z_3 = -1.0380887460967830$
$z_4 = 0.6234776317921379$	$z_5 = -1.1027532063031910$	$z_6 = -0.0141183222088869$
$y_1 = -1.6218101180868010$	$y_2 = 0.0061709468110142$	$y_3 = 0.8348493592472594$
$y_4 = -0.0511253369989315$	$y_5 = 0.5633782670698199$	$y_6 = -0.5$

Table 3: Coefficients for the $(7, 6, 4)$ processed splitting [2].

for the number of inner time steps

$$N = 1 + \left\lfloor \varepsilon^{-\frac{5}{8}} \sqrt{h} \right\rfloor.$$

This yields the desired generalized convergence rate $(7, 6, 4)$.

5.3 Processed Methods With Modified Potentials for Perturbed Systems

We split our Hamiltonian of interest (2.2) into a sum of the local quadratic part

$$\mathcal{A}(t) = -\tfrac{i}{\varepsilon^2}\left(T + M + U(x, t)\right)$$

at a position $q(t) \in \mathbb{R}^d$, and the non-quadratic remainder

$$\mathcal{B}(t) = -\tfrac{i}{\varepsilon^2} W(x, t).$$

This means, that for every fixed $t \in \mathbb{R}$, we have $V(x, t) = U(x, t) + W(x, t)$ with $U(x, t)$ the local quadratic Taylor expansion of $V(x, t)$ around $q(t)$. As mentioned above, $W(\cdot, t)$ perturbs the solution (w.r.t. $\mathcal{A}(t)$) by $\mathcal{O}(\varepsilon^3)$. Hence the theory of the previous sections applies, that is we interpret $\mathcal{B}(t)$ as a perturbation of order $\mathcal{O}(\varepsilon)$. Moreover, we have

$$\left[M(t), W(x, t)\right] \psi(x) = \left(M(t) W(x, t)\right) \cdot \psi(x)$$

for all smooth functions $\psi : \mathbb{R}^d \to \mathbb{C}$ and hence

$$\left[-\tfrac{i}{\varepsilon^2} W(x, t), \left[-\tfrac{i}{\varepsilon^2} M(t), -\tfrac{i}{\varepsilon^2} W(x, t)\right]\right] = 0. \tag{5.5}$$

On the other hand, we have [3, Sec. 3.4]

$$\left[-\tfrac{i}{\varepsilon^2}W(x,t),\left[-\tfrac{i}{\varepsilon^2}(T+U(x,t)),-\tfrac{i}{\varepsilon^2}W(x,t)\right]\right]=-\tfrac{i}{\varepsilon^2}\left(-\nabla_x W(x,t)\cdot\nabla_x W(x,t)\right).$$

The last two equations together yield

$$[\mathcal{B}(t),[\mathcal{A}(t),\mathcal{B}(t)]]=-\tfrac{i}{\varepsilon^2}\left(-\nabla_x W(x,t)\cdot\nabla_x W(x,t)\right).$$

This modified potential is exactly the same as in the zero magnetic field case in [3]. We can thus use the same modified propagator as proposed in [3, Sec. 3.5], namely

$$\varphi_{h,h/24}=\exp\left(h\mathcal{B}(t)+\frac{h^3}{24}[\mathcal{B}(t),[\mathcal{A}(t),\mathcal{B}(t)]]\right).$$

Here, we think of the time to be frozen at t. It can be evaluated at a similar computational cost as $e^{h\mathcal{B}}$, as explained in [3, Sec. 3.4]. Analogous to [3, Eq. (19)], we consider the method of generalized order $(6,4)$ from [2] given by

$$\Psi_{(6,4)}(h)=\left(e^{h\mathcal{B}}\overset{(y,z)}{\circ}e^{h\mathcal{A}}\right)\circ\left(e^{\frac{h}{2}\mathcal{A}}\circ\varphi_{h,h/24}\circ e^{\frac{h}{2}\mathcal{A}}\right)\circ\left(e^{-h\mathcal{A}}\overset{(z,y)}{\circ}e^{-h\mathcal{B}}\right),\tag{5.6}$$

with processing coefficients given in Table 4. This is basically a processed Strang splitting.

$y_1=-0.1659120515409654$	$y_2=-0.1237659000825160$	$y_3=0.0250397323738759$
$y_4=0.2269372219010943$		
$z_1=-0.9125829692505096$	$z_2=-0.3605243318856133$	$z_3=0.7354063037876117$
$z_4=0.5$		

Table 4: Coefficients for the $(6,4)$ processed splitting [2].

Consequently, this method is of similar computational cost as the semiclassical splitting, but provides highly improved accuracy. In Remark 2 we choose $\alpha=2$ and $\beta=4$, which yields for the number of inner time steps

$$N=1+\left\lfloor\sqrt{\tfrac{h}{\varepsilon}}\right\rfloor.$$

This yields the desired generalized convergence rate $(6,4)$.

5.4 Splitting Methods for Non-Autonomous Systems

Our problem can be written as a perturbed, non-autonomous system

$$\dot{\psi}(t)=\mathcal{A}(t)\psi(t)+\mathcal{B}(t)\psi(t),\quad \psi(t_0)=\psi_0$$

with

$$\mathcal{A}(t)=-\tfrac{i}{\varepsilon^2}(T+M(t)+U(x,t))\quad\text{and}\quad\mathcal{B}(t)=-\tfrac{i}{\varepsilon^2}W(x,t),$$

where $\mathcal{B}(t)$ is a perturbation of $\mathcal{A}(t)$ for small model parameters $\varepsilon>0$. In order to apply the theory discussed so far, we formulate an equivalent autonomous system by adding an additional component [3, Sec. 3]. This equivalent autonomous equation for $\psi=\psi(t)$ and $s=s(t)$ is given by

$$\partial_t\begin{pmatrix}\psi\\ s\end{pmatrix}=\begin{pmatrix}\mathcal{A}(s)\psi\\ 1\end{pmatrix}+\begin{pmatrix}\mathcal{B}(s)\psi\\ 0\end{pmatrix},\quad\psi(t_0)=\psi_0,\quad s(t_0)=t_0.$$

With $u = (\psi, s)$, we can rewrite the above evolution equation as

$$\dot{u} = \tilde{\mathcal{A}}(u) + \tilde{\mathcal{B}}(u),$$

where we introduce the vector fields

$$\tilde{\mathcal{A}} = \mathcal{A}(s)\,\tfrac{\delta}{\delta\psi} + 1 \cdot \tfrac{\delta}{\delta s} \quad \text{and} \quad \tilde{\mathcal{B}} = \mathcal{B}(s)\,\tfrac{\delta}{\delta\psi},$$

which act on functions $f(\psi, s)$, where $\frac{\delta}{\delta\psi}$ and $\frac{\delta}{\delta s}$ denote the (functional) derivatives with respect to the first and second argument of f. Our goal is to show that the commutator equations from the last subsection carry over to this extended setting, and thus also apply to the non-autonomous case. More precisely, we want to show that

$$\left[\tilde{\mathcal{B}}, \left[\tilde{\mathcal{A}}, \tilde{\mathcal{B}}\right]\right] = -\tfrac{i}{\varepsilon^2}\left(-\nabla_x W(x,s) \cdot \nabla_x W(x,s)\right)\tfrac{\delta}{\delta\psi}. \tag{5.7}$$

Fortunately, [3, Page 9] already yields

$$\left[\tilde{\mathcal{B}}, \left[-\tfrac{i}{\varepsilon^2}\left(T + U(x,s)\right)\tfrac{\delta}{\delta\psi}, \tilde{\mathcal{B}}\right]\right] = -\tfrac{i}{\varepsilon^2}\left(-\nabla_x W(x,s) \cdot \nabla_x W(x,s)\right)\tfrac{\delta}{\delta\psi}$$

and thus we only have to show

$$\left[\tilde{\mathcal{B}}, \left[-\tfrac{i}{\varepsilon^2} M(s)\tfrac{\delta}{\delta\psi}, \tilde{\mathcal{B}}\right]\right] = 0.$$

Indeed, for all suitable $f : C^\infty\left(\mathbb{R}^d\right) \times \mathbb{R} \to \mathbb{C}$, we have

$$\left[\tilde{\mathcal{B}}, \left[-\tfrac{i}{\varepsilon^2} M(s)\tfrac{\delta}{\delta\psi}, \tilde{\mathcal{B}}\right]\right] f(\psi, s) = \left[-\tfrac{i}{\varepsilon^2} W(x,t), \left[-\tfrac{i}{\varepsilon^2} M(t), -\tfrac{i}{\varepsilon^2} W(x,t)\right]\right]\tfrac{\delta^3}{\delta\psi^3} f(\psi, s) = 0,$$

where we used (5.5) for the last step. This proves (5.7). To summarize, we need to solve the autonomous equation (W frozen at time t_0)

$$\dot{\psi} = -\tfrac{i}{\varepsilon^2} W(x, t_0)\,\psi, \quad \psi(t_0) = \psi_0,$$

or in case of (5.6) the autonomous equation

$$\dot{\psi} = -\frac{i}{\varepsilon^2}\left(W(x,t_0) - \tfrac{h^2}{24}\nabla_x W(x,t_0) \cdot \nabla_x W(x,t_0)\right)\psi, \quad \psi(t_0) = \psi_0.$$

Furthermore, we need to solve the non-autonomous equation

$$\dot{\psi} = \mathcal{A}(t)\,\psi, \quad \psi(t_0) = \psi_0 \tag{5.8}$$

either exact or to high precision. The momentum part $T + M(t)$ needs to be split into

$$\partial_t \begin{pmatrix} \psi \\ s \end{pmatrix} = \begin{pmatrix} -\frac{i}{\varepsilon^2} T\psi \\ 0 \end{pmatrix} \quad \text{and} \quad \partial_t \begin{pmatrix} \psi \\ s \end{pmatrix} = \begin{pmatrix} -\frac{i}{\varepsilon^2} M(s)\,\psi \\ 1 \end{pmatrix}. \tag{5.9}$$

It is crucial to perform the evolution of $s(t)$ together with $M(s)$, so that the exact flow maps of the two equations commute. Their concatenation then yields the exact flow map of the momentum equation as in (5.9). The first equation in (5.9) is equivalent to (T) and the solution in terms of Hagedorn wavepackets can be computed explicitly, see Section 4, Item (i). It remains to approximate the solution of the second equation in (5.9), which is equivalent to Equation (M). This time, it cannot be solved by a simple matrix exponential due to the time dependence of $B(t)$. Instead, we apply a matrix expansion as explained in the next subsection.

5.5 Magnus Expansion for the Non-Autonomous Equation (M)

We recall that the PDE (M) can be reduced to the ODE

$$\tfrac{\mathrm{d}}{\mathrm{d}t} y(t) = B(t)\, y(t). \tag{B}$$

We approximate the exact flow $R(t, t_0) \in \mathrm{SO}(d)$ of (B) by a truncated Magnus expansion (see [19] or [16, Ch IV.7]). More precisely, we use in all subsequent simulations the following fourth order commutator free Magnus integrator from Example 1 in [5]. With nodes and weights

$$c := \begin{pmatrix} \frac{1}{2} - \frac{\sqrt{3}}{6} \\ \frac{1}{2} + \frac{\sqrt{3}}{6} \end{pmatrix}, \quad \alpha := \begin{pmatrix} \frac{1}{4} - \frac{\sqrt{3}}{6} \\ \frac{1}{4} + \frac{\sqrt{3}}{6} \end{pmatrix}.$$

and for a sufficiently small time step $\delta t > 0$, we define the orthogonal matrix

$$\tilde{R}(\delta t + t_0, t_0) := \exp(\alpha_1\, \delta t\, B_1 + \alpha_2\, \delta t\, B_2) \cdot \exp(\alpha_2\, \delta t\, B_1 + \alpha_1\, \delta t\, B_2), \quad B_j := B(c_j\, \delta t + t_0).$$

To solve (B) on a time interval $[t_0, t]$, we apply J steps of this scheme. More precisely, for a uniform time grid $t_j := t_0 + j\, \delta t$, where $j \in \{0, \ldots, J\}$ and $t = t_J$, we have

$$R(t, t_0) = \prod_{j=1}^{J} \tilde{R}(t_j, t_{j-1}) + \mathcal{O}\left((\delta t)^5\right).$$

As pointed out in [5], the fourth order convergence is due to [4, Eq (12)]. However, we want to avoid that the overall order of our splitting methods are dominated by this order 4 method. Since this truncated Magnus expansion is still much cheaper than the propagation w.r.t. $\mathcal{B}$, we can afford to solve (B) up to machine precision. For our simulations, this is done by choosing $J = 4096$ for all examples. Other examples might require different tuning. Just like in (2.4), we obtain an approximate solution of the PDE (M) by

$$\psi(x, t) = \psi_0\left(R^T(t, t_0)\, x\right) \approx \psi_0\left(\tilde{R}^T(t, t_0)\, x\right). \tag{5.10}$$

The approximation $\tilde{R}(t, t_0)$ lies in $\mathrm{SO}(d)$, which has two consequences [12]. First, this approximate time evolution is unitary. Second, it commutes with the kinetic operator T. Thus not only the exact, but even the approximate evolution operators factor like in (2.5).

6 Numerical Simulation

In the subsequent simulations we use a truncated Hagedorn wavepacket as in (3.3). The flow map $R(t, t_0) \in \mathrm{SO}(d)$ of (B), which is needed to solve (M), is approximated by the fourth-order commutator-free Magnus expansion as explained in Section 5.5. We plot the energies along the approximate solution $\tilde{u}(t)$ for unit charge and unit mass:

$$\begin{aligned}
E^{\varepsilon}_{\mathrm{kin}}(t) &:= \langle \tilde{u}(t), -\tfrac{\varepsilon^4}{2}\Delta \tilde{u}(t)\rangle_{L^2} && \text{(kinetic energy)} \\
E^{\varepsilon}_{\mathrm{mag}}(t) &:= \langle \tilde{u}(t), \left(H^{\varepsilon}_B(t) + \tfrac{1}{2}\|B(t)\, x\|^2_{\mathbb{R}^d}\right) \tilde{u}(t)\rangle_{L^2} && \text{(magetic energy)} \\
E_{\mathrm{pot}}(t) &:= \langle \tilde{u}(t), \phi(x)\, \tilde{u}(t)\rangle_{L^2} && \text{(potential energy)} \\
E^{\varepsilon}_{\mathrm{tot}}(t) &:= E^{\varepsilon}_{\mathrm{kin}}(t) + E^{\varepsilon}_{\mathrm{mag}}(t) + E_{\mathrm{pot}}(t). && \text{(total energy)}
\end{aligned}$$

The inner products in the definition of $E^{\varepsilon}_{\mathrm{kin}}$ and $E^{\varepsilon}_{\mathrm{mag}}$ can be computed just in terms of the coefficients. In case of a good approximate solution, we expect approximate conservation of total energy.

6.1 Penning Trap (single particle)

The following example is motivated by [17], where the authors propose a two-dimensional Penning trap [23, 6, 7] to implement qubits for experimental quantum computing. More precisely, their Penning trap confines ions in the plane spanned by the standard basis vectors $\vec{e}_1, \vec{e}_2 \in \mathbb{R}^3$, which normally requires a homogeneous magnetic field perpendicular to this plane, i.e. parallel to $\vec{e}_3 \in \mathbb{R}^3$. But in the actual experiment, this renders laser cooling infeasible. As a trade-off, one can choose the magnetic field to enclose a small angle $\Theta > 0$ with $\vec{e}_3$, see (6.2), so that laser cooling becomes feasible, while the magnetic field still traps the ions in the plane.[2] In our numerical experiments, we consider a particle of unit mass ($m = 1$) and unit charge ($e = 1$) in $d = 3$ dimensions. We use the time-independent Hamiltonian proposed in [17], namely

$$H^x_{\text{trap}} := -\tfrac{\varepsilon^4}{2}\Delta + H^\varepsilon_B + \tfrac{e^2}{2}\|Bx\|^2_{\mathbb{R}^3} + \phi_{\text{trap}}(x)$$

with $\varepsilon = 0.01$ and electric potential

$$\phi_{\text{trap}}(x) = \frac{1}{2}\left(x_3^2 - \frac{x_1^2 + x_2^2}{2}\right) \tag{6.1}$$

and a magnetic field $\vec{B}$ (now as vectorfield) enclosing the angle $\Theta = 0.4$ with $\vec{e}_3$, namely[3]

$$\vec{B} = 2\begin{pmatrix}\sin(\Theta)\\ 0\\ \cos(\Theta)\end{pmatrix}. \tag{6.2}$$

The corresponding vector potential is $\vec{A} = \frac{1}{2}\left(\vec{B} \times \vec{x}\right)$, which is represented by the time-independent skew-symmetric matrix

$$B = \begin{pmatrix} 0 & \cos(\Theta) & 0\\ -\cos(\Theta) & 0 & \sin(\Theta)\\ 0 & -\sin(\Theta) & 0\end{pmatrix}. \tag{6.3}$$

The initial data is given by $u(x,0) = \varphi_0^\varepsilon[\Pi(0)](x)$, where $\Pi(0) = (q,p,Q,P)$ and

$$q = (1,0,1), \quad p = (0,-1,0), \quad Q = \mathrm{id}, \quad P = i \cdot \mathrm{id}. \tag{6.4}$$

This corresponds to a particle that has, with high probability, a position near q and a momentum near p. In particular, it lies out of the equilibrium position of the trap (with high probability). Since the potential is quadratic, this corresponds to $\mathcal{A} = -\frac{i}{\varepsilon^2}H^x_{\text{trap}}$ and $\mathcal{B} = 0$ in the notation of the previous sections. It follows that we only need to propagate the parameters $\Pi(t)$ and $S(t)$, while the coefficients c_k remain constant. Therefore, we can choose $\mathcal{K} = \{(0,0,0)\}$ in (3.3). We use the semiclassical splitting from Section 4, i.e. Equation (4.2), with time step size $h = 0.01$. The energies along the approximate solution are shown in Figure 1. Note that the separate energies oscillate roughly between -2 and 2, while the energy drift varies at the scale of 10^{-4}. This means that the energy is conserved up to a small error.

[2] This explanation is simplified. For details, we refer to [17].

[3] Note that if $\Theta = 0$, the Hamiltonian H^x_{trap} can be separated into a (x_1, x_2)-part and a x_3-part. Thus the condition $\Theta > 0$ really renders the problem more complex.

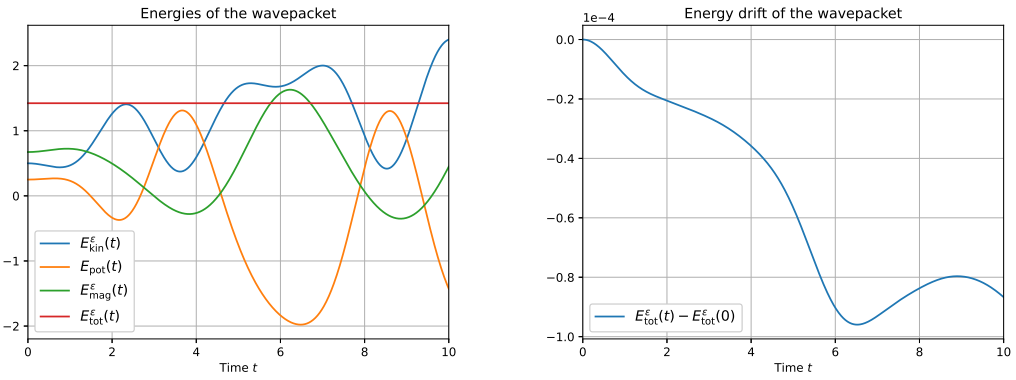

Figure 1: Single particle in a Penning trap. The total energy along the computed solution is approximately conserved. The separate energies $E^{\varepsilon}_{\mathrm{kin}}, E_{\mathrm{pot}}, E^{\varepsilon}_{\mathrm{mag}}, E^{\varepsilon}_{\mathrm{tot}}$ are defined at the beginning of Section 6. The solution was computed by the semiclassical splitting from Section 4. To reproduce the figure, see `examples/penning_trap_energies/` in the repository https://gitlab.math.ethz.ch/gvasile/WaveBlocksND.git.

6.2 Penning Trap (two particles)

We consider two charged particles of unit mass and charge in the same Penning trap as before. Thus we solve the Schrödinger equation in $d = 6$ dimensions. We write $x = \left(x^{(1)}, x^{(2)}\right) \in \mathbb{R}^3 \times \mathbb{R}^3$ for the coordinates of the particles. The repulsion between the particles is modeled by a Mie(4,2) potential [21], [12, Sec.3.5]

$$\phi_{\mathrm{rep}}\left(x\right) = 32 \cdot \left(\frac{3^4}{\|x^{(1)} - x^{(2)}\|^4_{\mathbb{R}^3}} - \frac{3^2}{\|x^{(1)} - x^{(2)}\|^2_{\mathbb{R}^3}} \right) + 8.$$

The Hamiltonian on $L^2\left(\mathbb{R}^6; \mathbb{C}\right)$ is then given by $H^{x^{(1)}}_{\mathrm{trap}} + H^{x^{(2)}}_{\mathrm{trap}} + \phi_{\mathrm{rep}}\left(x\right)$ or equivalently

$$-\tfrac{\varepsilon^4}{2}\Delta + H^{\varepsilon}_{B} + \tfrac{1}{2}\|Bx\|^2_{\mathbb{R}^6} + \phi\left(x\right),$$

where

$$\phi\left(x\right) = \phi_{\mathrm{trap}}\left(x^{(1)}\right) + \phi_{\mathrm{trap}}\left(x^{(2)}\right) + \phi_{\mathrm{rep}}\left(x\right) \quad \text{and} \quad B = \begin{pmatrix} B^{(1)} & 0 \\ 0 & B^{(2)} \end{pmatrix},$$

where $B^{(1)} = B^{(2)}$ are two copies of the matrix in (6.3). The initial data is chosen to be $\psi_0\left(x\right) = \varphi^{\varepsilon}_0\left[\Pi\left(0\right)\right]\left(x\right)$, where $\Pi\left(0\right) = \left(q, p, Q, P\right)$ and

$$q = (\underbrace{2, 0, 2}_{q^{(1)}}, \underbrace{0, -3, 0}_{q^{(2)}}), \quad p = (\underbrace{0, -1, 0}_{p^{(1)}}, \underbrace{0, 0, 1}_{p^{(2)}}), \quad Q = \mathrm{id}, \quad P = i \cdot \mathrm{id}\,.$$

Since the repulsion $\phi_{\mathrm{rep}}\left(x\right)$ is non-quadratic, we have to propagate also the coefficients $\left(c_k\left(t\right)\right)_{k \in \mathcal{K}}$ in (3.3). We use the fixed index set $\mathcal{K}$ as in (3.4) with $K = 6$. As before, we use the semiclassical splitting from Section 4, i.e. Equation (4.2), with time step size $h = 0.01$. The energies along the approximate solution are shown in Figure 2.
Note that the energy conservation is accurate at the beginning, but suddenly starts to worsen (at the scale of 10^{-4} though). This is a sign that the truncation constant $K = 6$ was chosen too small. Opposed to the previous example, we now have a non-quadratic remainder, i.e. the operator $\mathcal{B}$ does not vanish. It is also this operator that describes

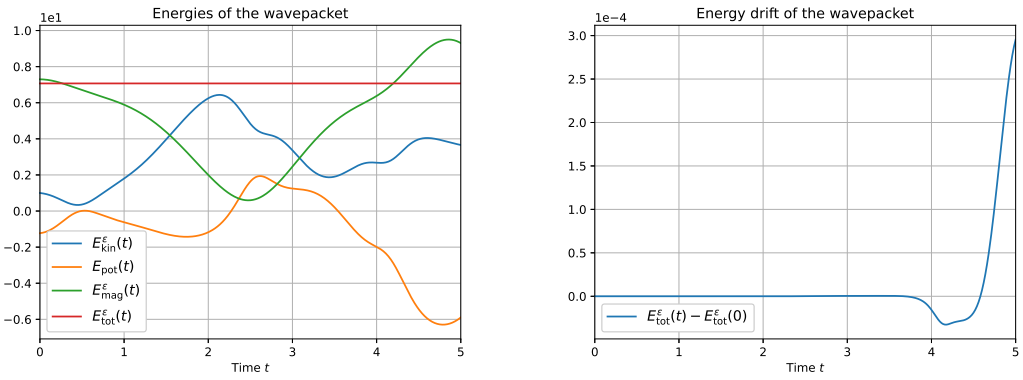

Figure 2: Two particles in the Penning trap. The total energy along the computed solution is approximately conserved. The separate energies $E^{\varepsilon}_{\mathrm{kin}}, E_{\mathrm{pot}}, E^{\varepsilon}_{\mathrm{mag}}, E^{\varepsilon}_{\mathrm{tot}}$ are defined at the beginning of Section 6. The solution was computed by the semiclassical splitting from Section 4. To reproduce the figure, see `examples/penning_trap_energies/` in the repository https://gitlab.math.ethz.ch/gvasile/WaveBlocksND.git.

the non-classical part of the time evolution. Beyond a certain time, the propagated wavefunction will deviate so much from the classical evolution that the coefficients $c_k, k \in \mathcal{K}$ cannot account for this deviation anymore. Put differently, the solution flows out of the subspace of $L^2\left(\mathbb{R}^d\right)$ spanned by the $\varphi^{\varepsilon}_k, k \in \mathcal{K}$. This maximal propagation time can be extended by choosing a larger truncation constant K. For an error plot for different values of K we refer to [11, Fig. 5]. This issue is also closely related to the Ehrenfest time [8].

6.3 Convergence of the Different Splittings

We analyse the convergence in time and for different model parameters $\varepsilon > 0$. Moreover, we summarize the theoretical considerations from Section 5 in Table 5. The latter is exactly the same as Table 3 in [3], since even with the new magnetic terms, the bottleneck of all methods is still the propagation according to the non-quadratic remainder (the operator $\mathcal{B}$ in the notation of Section 5).

Method	Type	Cost	Order
(4.2)	semiclassical	1	εh^2
(5.2)	perturbed	2	$\varepsilon h^4 + \varepsilon^2 h^4$
(5.3)	perturbed	5	$\varepsilon h^8 + \varepsilon^2 h^4$
(5.4)	perturbed, processor	3	$\varepsilon h^7 + \varepsilon^2 h^6 + \varepsilon^3 h^4$
(5.6)	perturbed, processor, modification	1	$\varepsilon h^6 + \varepsilon^2 h^4$

Table 5: Comparison of the different splitting methods.

For the convergence plots below, we use a single particle in $d = 3$ dimensions, subject to a Morse potential

$$\phi_{\mathrm{Morse}}(x) = 8 \cdot \left(\exp\left(-2 \cdot 0.3 \cdot \left(\|x\|_{\mathbb{R}^3} - 4\right)\right) - 2 \cdot \exp\left(-0.3 \cdot \left(\|x\|_{\mathbb{R}^3} - 4\right)\right)\right) + 8.$$

the magnetic field is given by

$$B(t) = \begin{pmatrix} 0 & \cos(\pi t) & 0 \\ -\cos(\pi t) & 0 & \sin(\pi t) \\ 0 & \sin(\pi t) & 0 \end{pmatrix}.$$

We solve the Schrödinger equation on the time interval $[0, 2]$ with initial data $\psi_0(x) = \varphi_0^\varepsilon[\Pi(0)](x)$, where $\Pi(0) = (q, p, Q, P)$ is the same as in (6.4). The index set $\mathcal{K}$ in (3.4) is truncated by $K = 32$ for both the approximate and the reference solution. The latter was computed with the modified potential splitting (5.6) of time steps of size $h = 2^{-6}$. The plots in Figures 3, 4, 5, 6, 7 show the L^2-difference to reference solution at final time $T = 2$. The L^2-norm was computed by a scaled and very accurate Gauss-Hermite quadrature as described in [9, Sec.4.1]. The results are qualitatively the same as for the standard Schrödinger equation in [11, Fig.5]. In particular, the methods improve for small values of ε. To reproduce the figures, run the files in `examples/penning_trap_convergence/` in the repository https://gitlab.math.ethz.ch/gvasile/WaveBlocksND.git.

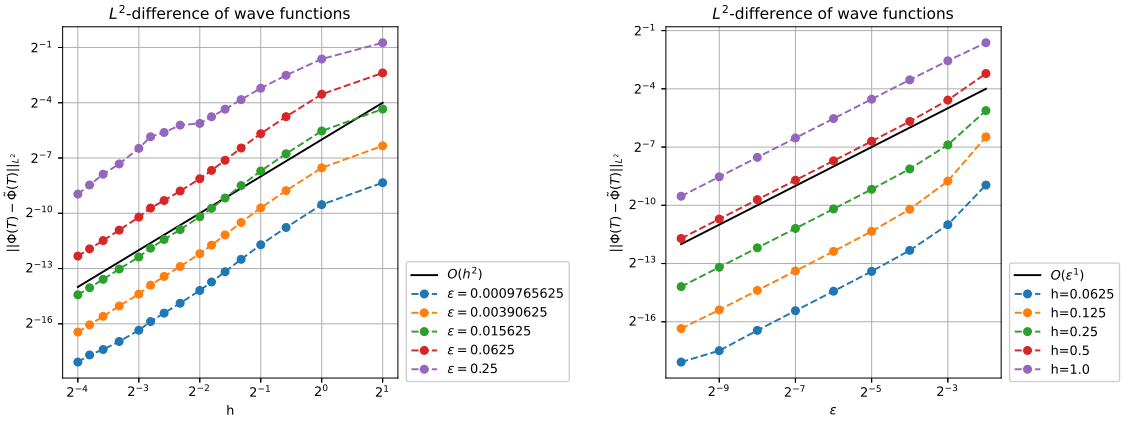

Figure 3: Semiclassical splitting of order 2 as described in Section 4.

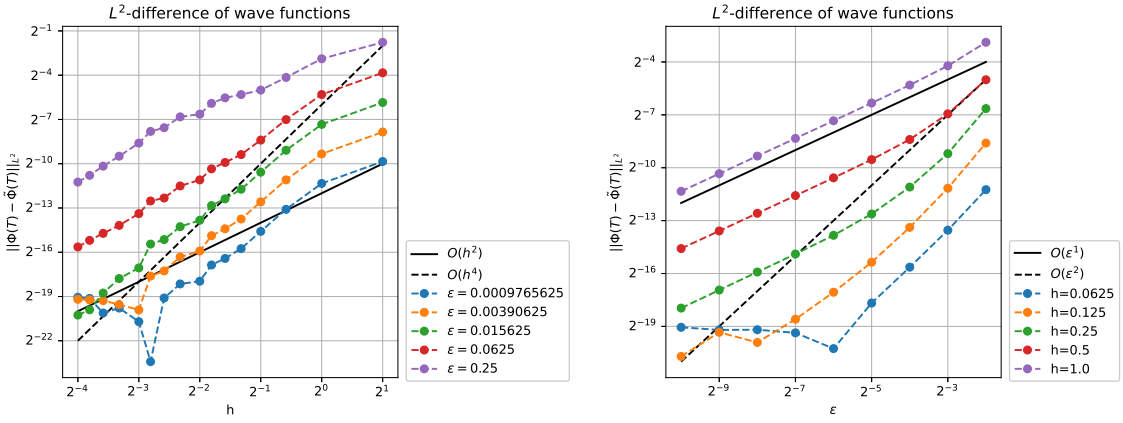

Figure 4: Perturbation-aware splitting of generalized order $(4, 2)$ as described in Section 5.1.

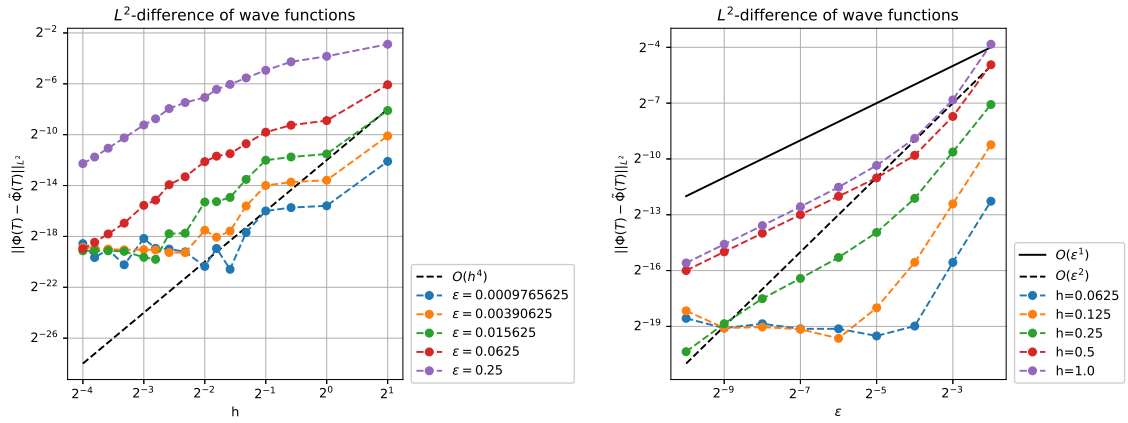

Figure 5: Perturbation-aware splitting of generalized order $(8, 4)$ as described in Section 5.1. The splitting coefficients are given in Table 2.

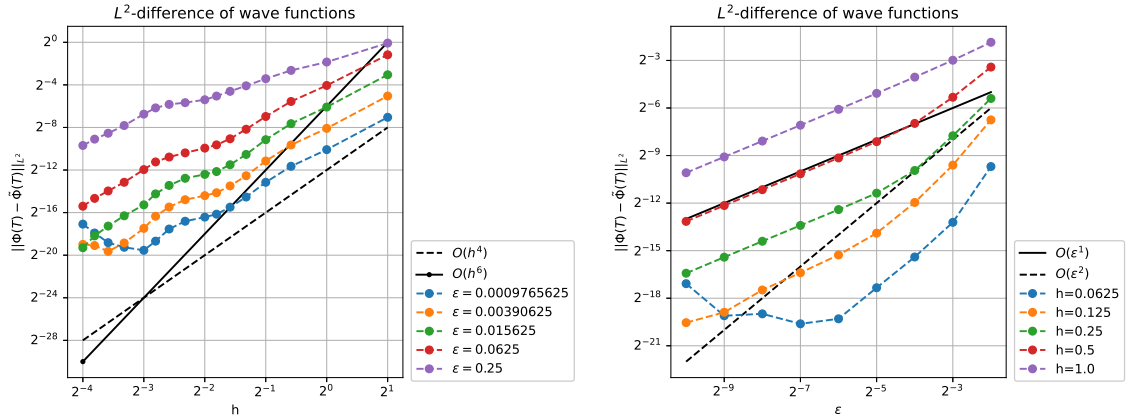

Figure 6: Perturbation-aware processed splitting of generalized order $(7, 6, 4)$ as described in Section 5.2. The splitting coefficients are given in Table 3.

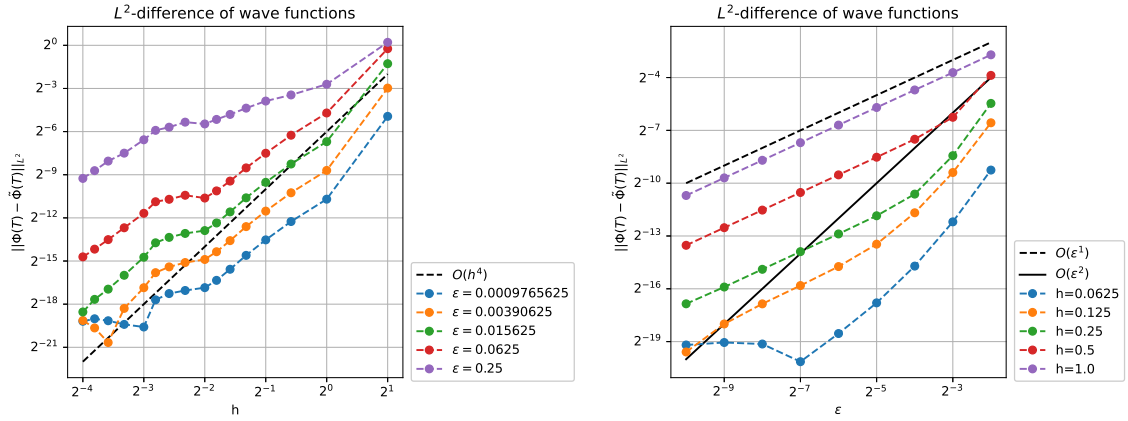

Figure 7: Perturbation-aware processed splitting with modified potential of generalized order $(6, 4)$ as described in Section 5.3. The splitting coefficients are given in Table 4.

References

[1] Sergio Blanes and Fernando Casas. *A concise introduction to geometric numerical integration*. Chapman & Hall/CRC Monographs and Research Notes in Mathematics. CRC Press, 2017.

[2] Sergio Blanes, Fernando Casas, and J. Ros. Processing symplectic methods for near-integrable Hamiltonian systems. *Celestial Mechanics and Dynamical Astronomy*, 77:17–36, 07 2000.

[3] Sergio Blanes and Vasile Gradinaru. High order efficient splittings for the semi-classical time–dependent Schrödinger equation. *Journal of Computational Physics*, 405:109157, 2020.

[4] Sergio Blanes and Per Christian Moan. Splitting methods for the time-dependent Schrödinger equation. *Physics Letters A*, 265(1):35 – 42, 2000.

[5] Sergio Blanes and Per Christian Moan. Fourth- and sixth-order commutator-free Magnus integrators for linear and non-linear dynamical systems. *Applied Numerical Mathematics*, 56(12):1519 – 1537, 2006.

[6] Lowell S. Brown and Gerald Gabrielse. Geonium theory: Physics of a single electron or ion in a Penning trap. *Rev. Mod. Phys.*, 58:233–311, Jan 1986.

[7] Hans Dehmelt. A single atomic particle forever floating at rest in free space: New value for electron radius. *Physica Scripta*, T22:102–110, jan 1988.

[8] P. Ehrenfest. Bemerkung über die angenäherte Gültigkeit der klassischen Mechanik innerhalb der Quantenmechanik. *Zeitschrift fur Physik*, 45(7-8):455–457, July 1927.

[9] Erwan Faou, Vasile Gradinaru, and Christian Lubich. Computing semiclassical quantum dynamics with Hagedorn wavepackets. *SIAM J. Scientific Computing*, 31:3027–3041, 01 2009.

[10] Luigi Galati and Shijun Zheng. Nonlinear Schrödinger equations for Bose-Einstein condensates. *AIP Conference Proceedings*, 1562:50–64, 10 2013.

[11] Vasile Gradinaru and George A. Hagedorn. Convergence of a semiclassical wavepacket based time-splitting for the Schrödinger equation. *Numerische Mathematik*, 126(1):53–73, Jan 2014.

[12] Vasile Gradinaru and Oliver Rietmann. A high-order integrator for the Schrödinger equation with time-dependent, homogeneous magnetic field. *The SMAI journal of computational mathematics*, 6:253–271, 2020.

[13] George A. Hagedorn. Semiclassical quantum mechanics. i. the $\hbar \to 0$ limit for coherent states. *Comm. Math. Phys.*, 1(1):77–93, 1980.

[14] George A. Hagedorn. Raising and lowering operators for semiclassical wave packets. *Annals of Physics*, 269(1):77 – 104, 1998.

[15] Ernst Hairer, Christian Lubich, and Gerhard Wanner. *Geometric numerical integration: Structure-preserving algorithms for ordinary differential equations*, volume 31 of *Springer series in computational mathematics*. Springer, Berlin, second edition, 2010.

[16] Brian C. Hall. *Quantum theory for mathematicians*, volume 267 of *Graduate texts in mathematics*. Springer, New York, 2013.

[17] Shreyans Jain, Joseba Alonso, Matt Grau, and Jonathan P. Home. Quantum simulation with ions in micro-fabricated Penning traps. *arXiv e-prints*, page arXiv:1812.06755, Dec 2018.

[18] William Kahan and Ren-Cang Li. Composition constants for raising the orders of unconventional schemes for ordinary differential equations. *Mathematics of Computation*, 66:1089–1099, 1997.

[19] Wilhelm Magnus. On the exponential solution of differential equations for a linear operator. *Communications on Pure and Applied Mathematics*, 7(4):649–673, 1954.

[20] Robert I. McLachlan. Composition methods in the presence of small parameters. *BIT*, 35(2):258–268, 1995.

[21] Gustav Mie. Zur kinetischen Theorie der einatomigen Körper. *Annalen der Physik*, 316(8):657–697, 1903.

[22] Wolfgang Pauli. Zur Quantenmechanik des magnetischen Elektrons. *Zeitschrift für Physik*, 43(9):601–623, Sep 1927.

[23] F.M. Penning. Die Glimmentladung bei niedrigem Druck zwischen koaxialen Zylindern in einem axialen Magnetfeld. *Physica*, 3(9):873–894, 1936.

[24] Barry Simon and Michael Reed. *Fourier analysis, self-adjointness*, volume 2 of *Methods of modern mathematical physics*. Academic Press, Boston, 1975.

[25] Gilbert Strang. On the construction and comparison of difference schemes. *SIAM Journal on Numerical Analysis*, 5:506–517, 1968.

[26] Zhennan Zhou. Numerical approximation of the Schrödinger equation with the electromagnetic field by the Hagedorn wave packets. *Journal of Computational Physics*, 272:386–407, 09 2014.